Bond behavior of PP fiber-reinforced cinder concrete after fire exposure

Bin Cai [ab], Ansheng Wu[a] , Feng Fu [b]

[a] School of Civil Engineering, Jilin Jianzhu University, Changchun, 130118, China
[b].School of Mathematics, Computer Science and Engineering, City, University of London, London, EC1V 0HB,UK

Abstract. To reduce the damage of concrete in fire, a new type of lightweight cinder aggregate concrete was developed due to the excellent fire resistance of cinder. To further enhance its fire resistance, Polypropylene (PP) Fibers which can enhance the fire resistance of concrete were also used in this type of concrete. However, the bond behavior of this new type of concrete after fire exposure is still unknown. To investigate its bond behavior, 185 specimens were heated up to 22, 200, 400, 600 or 800 ºC for 2 h duration respectively, which is followed by subsequent compressive and tensile tests at room temperature. The concrete-rebar bond strength of C30 PP fiber-reinforced cinder concrete was subsequently investigated through pull-out tests after fire exposure. The microstructures of the PP fiber-reinforced cinder concrete and the status of the PP fibre at different temperature were inspected using an advanced scanning electron microscopy, aiming to understand the mechanism of the bonding deterioration under high temperature. The effects of rebar diameter and bond length on the bond strength of PP fiber-reinforced cinder concrete were investigated based on the test results. The bond-slip relation of PP fiber-reinforced cinder concrete after exposure at different temperature was derived based on the test results.

Keywords: Cinder, Bond strength, fire performance PP fibre, Fire test

1. Introduction

In practical engineering applications, the bond strength between rebar and concrete matrix significantly affects the mechanical properties of reinforced concrete structures (Huang et al, 2016). The complete bonding between rebar and concrete matrix ensures the stress transfer and the homogeneous deformation, and thereby eliminates the local structure failure under the designed load (Fu 2016a, Ma et al, 2019; Pothisiri and Panedpojaman, 2010). However, due to the lack of sufficient bonding or embedment length in practical application, debonding may occur sometimes, especially at the location of shearing force concentration (Ding et al, 2014).

Fire would severely threaten the life and possessions of humans (WU and TANG, 2010; ZHENG et al, 2011, Fu 2015, Fu 2016b, Fu 2018). In particular, the most frequently-occurring one is building fire, which would cause huge losses and thus become the focus of scholars (Adnan et al, 2010; Kang, 2017; Tang, 2017; Bidgoli and Saeidifar, 2017; Alireza and Gholamreza, 2019; Moetaz, 1996; Hamed and Masood, 2019; Lü et al, 2012). The mechanical properties of both rebar and concrete (YANG, 2014; SHEN, 1991; Gulsan, 2018) and the bonding between rebar and concrete would be significantly reduced after fire (El-Hawary, 1997, Lie, 1994). Since the rebar-concrete bonding force is the major cause for the engagement of the two different materials so, the deterioration of rebar-concrete bond in fire largely affects the bearing capacity (Pothisiri and Panedpojaman, 2010), Therefore, it is imperative to study the rebar-concrete bonding performance and assess the mechanical properties of reinforced concrete structures under fire.

The bond force of reinforced concrete under high temperature has been tested through pull-out tests or extrusion tests (Xiao et al. 2014; Royles and Morley, 1985; Varona, 2018). Researchers studied the bond strengths between round rebar or deformed steel and concrete under high temperature (Hertz, 1982; Royles and Morley, 1983). EI-Hawary et al. (1996) studied the effects of natural cooling and soaking cooling on the high-temperature bond strength (Ahmed, 1992). Diederichs & Schneider (1981) and Morley & RoyIes (1983) investigated the high-temperature rebar-concrete bond strength through pull-out tests. Haddad (2008) explored the high-temperature bond strength between fiber concrete and rebar and presented the equation. Through acoustic transmission and pullout tests, Chiang and Tsai (2000) concluded the equation to calculate the reduction factor of post-fire rebar-concrete bond strength. Generally, the cause of bond strength is mainly related to chemical bonding, the mechanical interlock between deformed steel rib and the concrete, and the friction after the rebar-concrete debonding (Yoo et al, 2015; Pothisiri and Panedpojaman, 2015). Before the debonding, the bond strength is mainly caused by the mechanical interlock by deformed steels, but the mechanical strength of concrete is important (Ganesan et al, 2014; Yang et al, 2016). Thus, the bond strength can be effectively improved by enhancing the mechanical strength of concrete. However, the obvious reduction in the mechanical strength of concrete at high temperature (Xiao et al, 2016; Pineaud et al, 2016) would decrease bond strength, high-performance concrete should be developed to meet engineering requirements.

In recent years, various high-performance porous lightweight concrete has been developed to reduce self-weights of the structure and enhance structural strength and insulation performances (Thomas, 2003; Wang, 2003;

Behnam and Shami, 2017). For instance, ultra-high-performance lightweight concrete (UHPLC) is designed with fly ash as the light aggregate to reduce weight (Wang, 2013), while foamed concrete contains numerous sealed pores that contribute to enhance fireproof and heat preservation performances (Liu et al. 2017, Jones and McCarthy, 2005; Ramamurthy, 2009).

Although the high porosity leads to the relatively low strength, complex construction processes, and high costs in the majority of lightweight concretes, porous PP fiber-reinforced cinder concrete has high research values owing to its high anti-cracking ability, lightweight and particularly the high-temperature resistance (Li, 2018; YANG, 2017). and cheap price.

Nevertheless, its post-fire mechanical properties have been rarely studied, and the bonding ability between PP fiber-reinforced cinder concrete and rebar after fire has not been investigated. Thus, this study will considerably contribute to the further application of this new type of PP fiber-reinforced cinder concrete. This study was mainly aimed to study the bonding behaviors between rebars and PP fiber-reinforced cinder concrete and further to analyze the effects of temperature on their bond strength. The research team made a pre-investigation on the mixture ratio (Fan, 2015), for fiber-reinforced lightweight aggregate concrete composite material in view of the practical application The bonding behavior between reinforced bar, and then analysis the influence of different temperature on the bonding strength will be further investigated in this paper. In brief, an exclusive temperature heating device and a loading device were designed and manufactured, and the bond strength deterioration between rebar and concrete was explored through pull-out test. The tested variables included temperature, rebar diameter and embedment length. Totally 185 specimens were made, including 10 standard specimens and 27 pull-out specimens without heat treatment, 40 standard specimens and 108 pull-out specimens after heated for 2 h at four different temperatures. The mechanical properties and microstructures of PP fiber-reinforced cinder concrete before and after fire exposure were studied, and finally the bond strength variation between PP fiber-reinforced cinder concrete and rebars after fire was explored. This work is expected to offer some insights into the feasibility of real application of porous PP fiber-reinforced cinder concrete components under fire.

2. Fire test of reinforced PP fiber-reinforced cinder concrete

2.1 Materials and compositions

The concrete was casted using cinder aggregate, ordinary Portland cement, fly ash (grade II), polypropylene (PP) fiber, styrene-acrylate emulsion, and water (Table 1). The porous cinder aggregate was collected from Guzhanzi in Huinan County (Fig. 1a), Jilin province, which has abundant cinder resources. The cinder was featured by packing density of 815 kg/m^3, lightweight, high porosity and low thermal conductivity. Polypropylene (PP) Fibers have been used in most of the tunnel project for their ability to reduce spalling in concrete under fire, by allowing moisture and water vapour to escape as the temperature of concrete exposed to a fire increase. To enhance the fire resistance of this new type of concrete, 9 mm long PP fibers were added into the concrete mix with tensile strength of 400 MPa and melting point at 160 ºC (Fig. 1b). The research team has developed and studied the properties of this fiber-reinforced lightweight aggregate cement composite for scoria aggregate (Fan, 2015), different aspects of PP fiber-reinforced cinder concrete, such as dosage of PP fiber has been investigated. According to the existing test results, through the preliminary experiments, it is found that the 1.0 ‰. of PP fiber dosage is most appropriate. The newly prepared PP fiber-reinforced cinder concrete had strength up to C30 grade and reached the average density of 1800 kg/m^3.

Table1 Preparation of PP fiber-reinforced cinder concrete

Material	Cinder aggregate	Ordinary Portland cement	Grade II fly ash	PP fibers	Styrene- acrylate emulsion	Water
Ratio	1800	1000	100	1	10	770
Dose (kg)	550	305.6	30.6	0.3	3	235.3

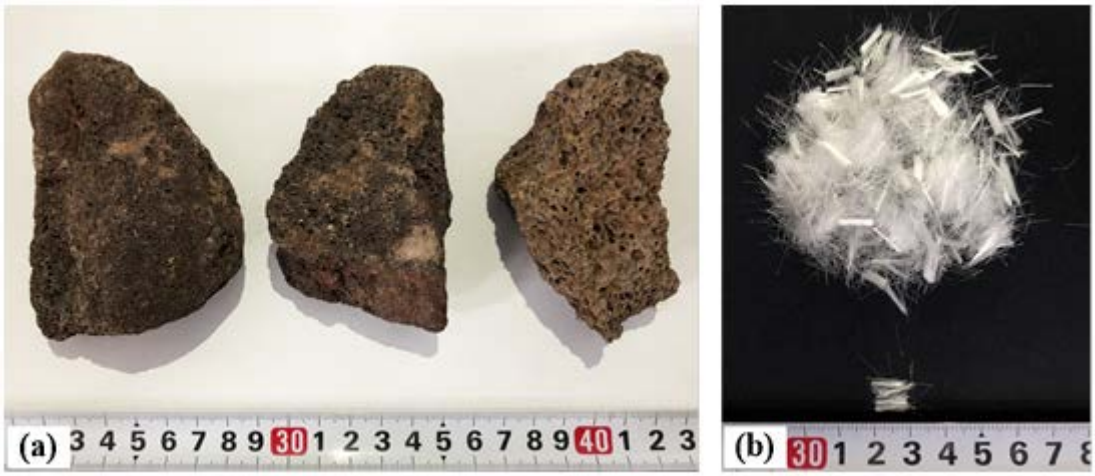

Fig. 1. Appearance of the materials used(a)Natural Cinder aggregate(b)Polypropylene Fibers.

2.2 Mechanical properties and microstructures of materials

Before the debonding between deformed steels and concrete, the bond strength is mainly due to the mechanical interlock effect between them and is dominated by the mechanical strength of concrete (Ganesan et al, 2014; Yang et al, 2016). When the deformed steels are pulled, the tensile force generates shear stress on the contact concrete through the side ribs of the deformed steels, and the mechanical interlocking effect laterally constrains the deformed steels to be pulled out (Ma, 2019; Pothisiri and Panedpojaman, 2012). Thus, in this paper, the compressive strength and tensile strength of PP fiber-reinforced cinder concrete were tested before and after fire exposure, aiming to clarify how the changes of concrete mechanical properties would affect the bond strength.

The PP fiber-reinforced cinder concrete standard specimens (150 ×150 ×150 mm^3) were made for axial compressive strength test and splitting tensile strength test. The first test was compression test (Fig. 2a) at the loading rate of 0.5 MPa/s, and the same batch of specimens were used in the tensile strength test (Fig. 2b) at the same pressure tester at the rate of 0.05 MPa/s. The splitting tensile strength (f_t, MPa) was calculated as follows (GB, 2010; GB/T, 2002):

$$f_t = \frac{2F}{\pi A} \quad (1)$$

where F is the failure load (N) and A is the area of the split surface (mm^2).

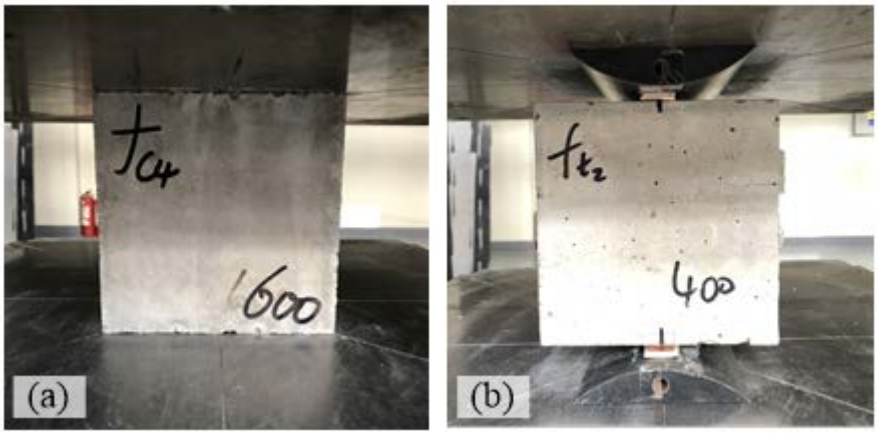

Fig. 2. Cubic concrete
strength test(a)Axial compressive strength test, (b) Tensile Splitting tensile strength test.

Totally 50 cubic concrete specimens were made, which were equally divided for the two tests. In brief, after pouring, the specimens were preserved at room temperature (22 ºC) for 24 h, and then de-molded and solidified at relative humidity 95±5% at room temperature until the 28th day. The specimens were divided into 5 groups (each 10 specimens) according to heating temperature, including room temperature (RT), 200, 400, 600 and 800 ºC. Firstly, the specimens were dried in oven at 100 ºC for 24 h, and then heated in a computer-controlled electric oven at the rate of 10 ºC/min until reaching the target temperature (Fig. 3).

After maintaining at the target temperature for 2 h, the specimens reached a thermal steady state, and then naturally cooled to the ambient temperature for the compressive strength and splitting tensile strength tests (Fig. 4).

Fig. 3 Electric oven for heating

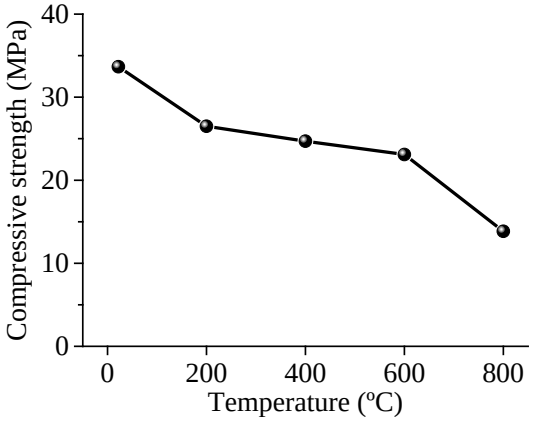

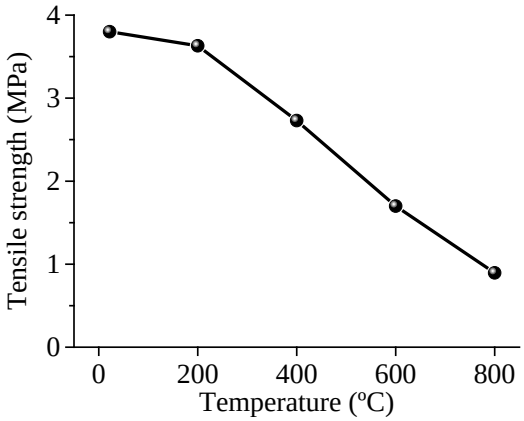

Fig. 4. Compressive strength and splitting tensile strength after temperature exposure

With the temperature rising from 22 to 200 ºC, the average compressive strength was reduced by 21.27% from 33.66 to 26.5 MPa. With a further rising temperature, the compressive strength was further weakened due to dehydration and decomposition of hydrates. The average compressive strength declined to 13.85 MPa at above 800 ºC. The properties of concrete including splitting tensile strength and ductility were weakened at the high temperature. With the temperature rising from 22 to 800 ºC, the splitting tensile strength was reduced by 74.43% from 3.5 to 0.895 MPa.

To investigate the microstructure of the concrete, the microstructures of the post-fire specimens were observed under scanning electron microscopy (SEM, TESCAN, MIRA3, made in Czech Republic)(Fig. 5a).Scanning electron microscopy (SEM) is widely used in the research of metal materials (steel, metallurgy, non-ferrous, mechanical processing) and non-metallic materials (chemical, chemical industry, petroleum, geological mineralogy, rubber, textile, cement, fiberglass). The fragments of the fractured specimens were inspected at room temperature first as a control result. It could be clearly observed from the figure 5b that the microstate of PP fiber was intact at room temperature , and the contact situation with concrete could be observed (Fig. 5b, c)， Due to the low thermal conductivity of PP fiber-reinforced cinder concrete, some PP fibers were still observed in the specimens after the heat treatment at 200 ºC, although the melting point of PP fibers is 165 ºC(Fig. 5d, e). However, when the temperature rose to 400, 600 and 800 ºC, the PP fibers disappeared, leaving some channels in the concrete matrix (Fig. 5g, h, l). The channels can let vapor to escape, therefore reduce pore pressure, thus reduce the spalling of the concrete. However, the tensile strength and bond strength of the concrete specimens further decreased. Thus, the strength of PP fiber-reinforced cinder concrete after 400 ºC temperature reduces.

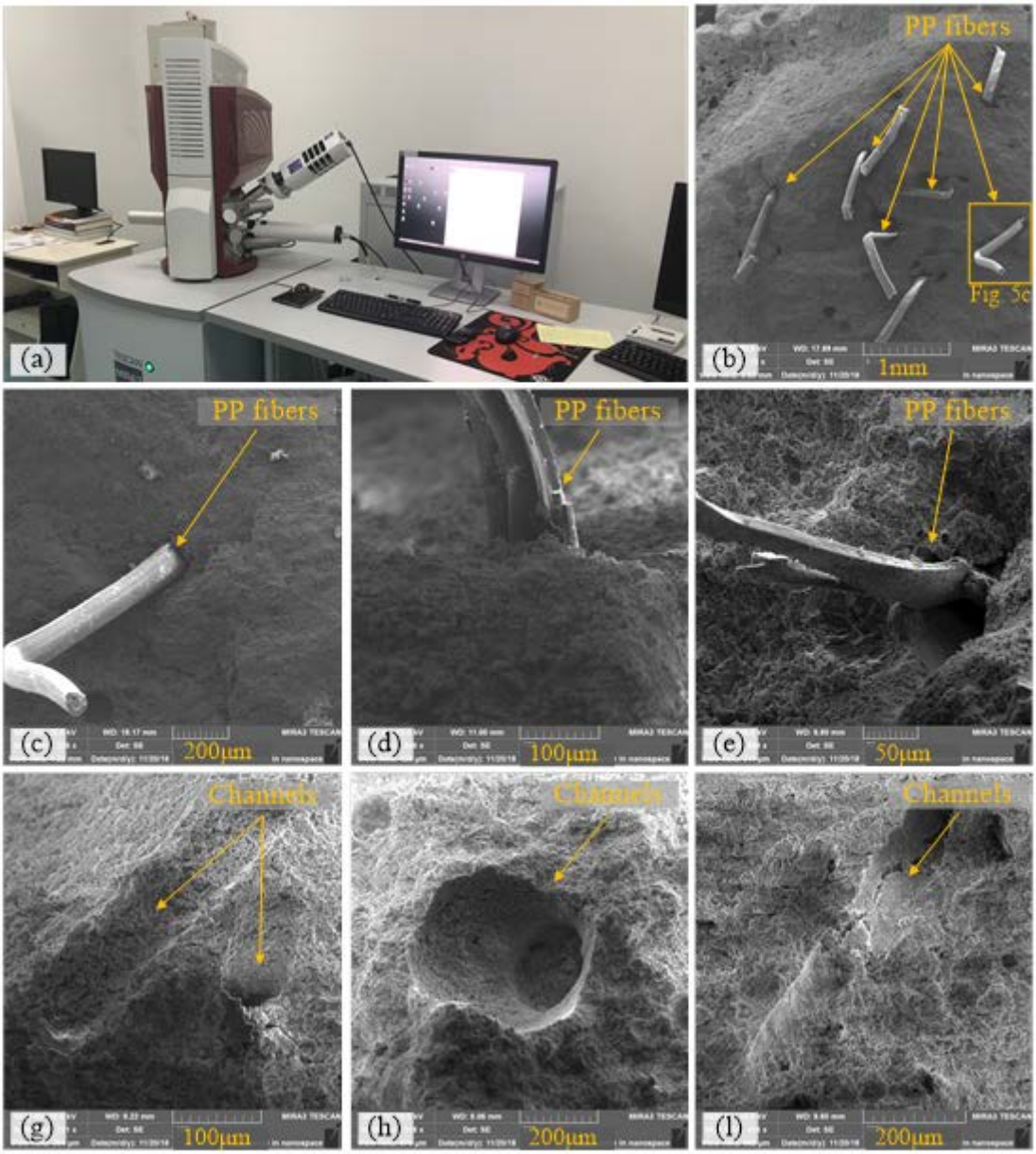

Fig. 5 Microstructures of PP fiber-reinforced cinder concrete with pp fibre after heat treatment (a)Scanning electron microscopy (b)22 ℃ microstructure (c)22 ℃ microstructure (d)200 ℃ microstructure (e)200 ℃ microstructure (g)400 ℃ microstructure (h)600 ℃ microstructure (l)800 ℃ microstructure

3. Pull-out tests

3.1 Test Specimen

As it shown in Fig.6, deformation rebars were embedded into the PP fiber-reinforced cinder concrete cubes (150 ×150 ×150 mm^3) with the two ends exposed, the anchorage length of the rebars was controlled by polyvinyl chloride (PVC) soft tubes (Fig. 6a, b). The concrete casting and curing following the conventional methods (Fu,2010,2008).The specimens embedded with deformed steels were shown in Fig. 6c. As for the specimens heated at high temperature, the sudden temperature rising of rebars would cause significant increase in the inner temperature gradient and inner stress, thereby leading to concrete burst (KODUR, 2003; 2004; XIAO and FALKNER, 2006). Thus, to avoid such burst and the consequent impact on the test data, the rebars before heat treatment were firmly coated with 50-mm-thick fireproof cotton. Some specimens were shown in Fig. 6e.

Another 135 pull-out specimens were made with the same batch of concrete pouring and the same curing condition (Fig. 6f). Deformed steels in three different diameters of 16, 20 and 24 mm were used. Three contact lengths were used, including 50, 70 and 90 mm. Each condition was tested with 3 specimens to analyse the variability.

The pull-out specimens were divided into 5 groups (each with 27 specimens) According to the heating temperature. A set of samples at ambient temperature

without heat treatment, the other four groups of samples at 200 ℃, 400 ℃, 600 ℃ and 800 ℃ under the temperature of heat treatment. After the heat treatment, the specimens were reserved in the oven until cooled to room temperature.

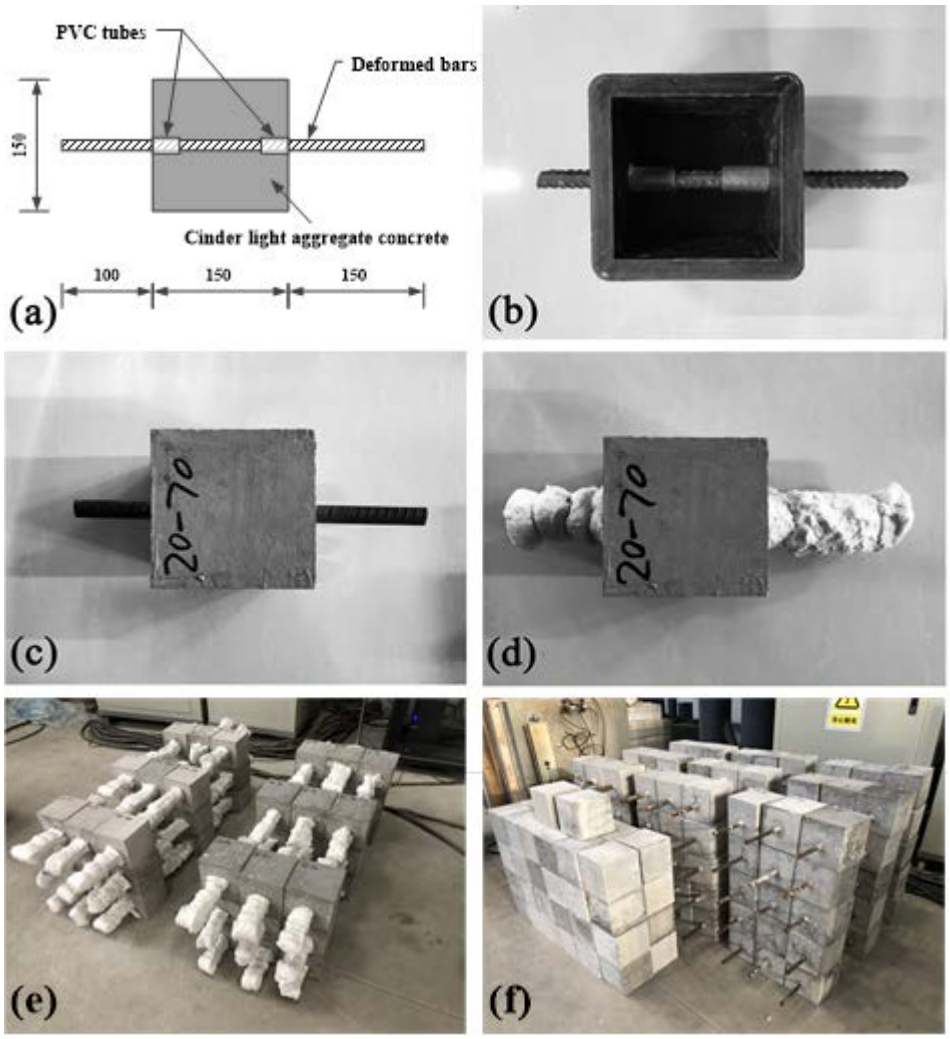

Fig. 6. Specimens for pull-out test (unit: mm). (a) Dimension drawing of test block (b) Test block mold (c) Finished test block (d) test block after fireproof cotton treatment (e) part of test block after fireproof cotton treatment (f) all test blocks

Table 2 listed the rebar diameters, anchorage length, and heating conditions. The specimens were denoted as C-a-b, where C represents the type of concrete, a is the rebar diameter, and b is the embedment length (for instance, C-16-50 means PP fiber-reinforced cinder concrete inserted with 16-mm-diameter rebar, and the contact length is 50 mm). The inner rebars were all HRB400 rebars of China (GB, 2007), where HRB400 means screw thread rebar with yield strength of 400 MPa. In engineering, HRB400 is used as longitudinal rebar for structure components that require for high bearing capacity.

Table 2 Classification of specimens

Designation	Rebar type	Rebar diameter (mm)	Embedment length (mm)
C-16-50	HRB400	16	50
C-16-70	HRB400	16	70
C-16-90	HRB400	16	90
C-20-50	HRB400	20	50
C-20-70	HRB400	20	70
C-20-90	HRB400	20	90
C-24-50	HRB400	24	50
C-24-70	HRB400	24	70
C-24-90	HRB400	24	90

3.2 Test setup

The similar instrumentation of the tests (Fu,2010, Gao,2017, Qian 2020 and Wen 2020,Deng,2020,Guo,2019) was adopted. The pull-out tester was illustrated in Fig. 7. Each specimen was restrained by a steel frame, which consisted of two 30-mm-thick rebar plates and five 25-mm-diameter rebar bars. The frame was clamped by an MTS (Maximum test force: 2000KN, indication accuracy: <1%, motor power: 0.75kW, operating voltage: 380V/220V) loading frame. The rebars of a specimen passed through the reserved hole on the lower plate and was clamped by the lower clamping device. Lubricating oil was painted in between each specimen and the bottom plate, so as to reduce the specimen-rebar friction during the pull-out tests. Two displacement meters were installed on the top of each specimen to measure the relative slip of the rebar to the specimen, and the pull force was recorded by the force meter of the loading frame. The bond strength of PP fiber-reinforced cinder concrete was calculated as follows:

$$\tau = \frac{P}{\pi dl} \tag{2}$$

where P is the peak pull force (N), d is the rebar diameter (mm), and l is the embedment length of rebars (mm).

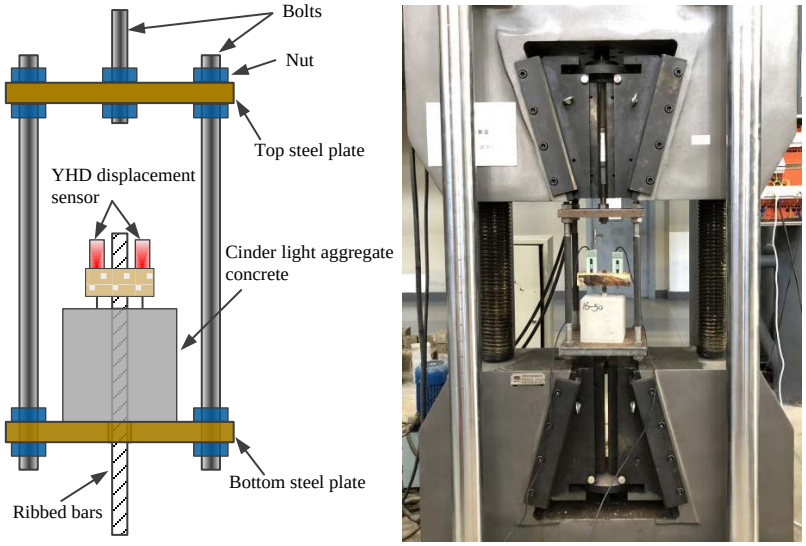

Fig. 7 Pull-out experimental installation

4. Experimental results

4.1 Phenomenon observation

The failure modes of PP fiber-reinforced cinder concrete were divided into shear failure, shear-split failure, and split failure (Fig. 8a-c). The shear failure means no evident cracks are left on the specimen bottom when the rebars are pulled out (Fig. 8a). The shear-split failure indicates the specimen remains as a whole, but evident cracks appear on the bottom during the pull-out (Fig. 8b). During the split failure, when the rebars are pulled out, evident cracks appear on the bottom and the specimen splits into parts (Fig. 8c).

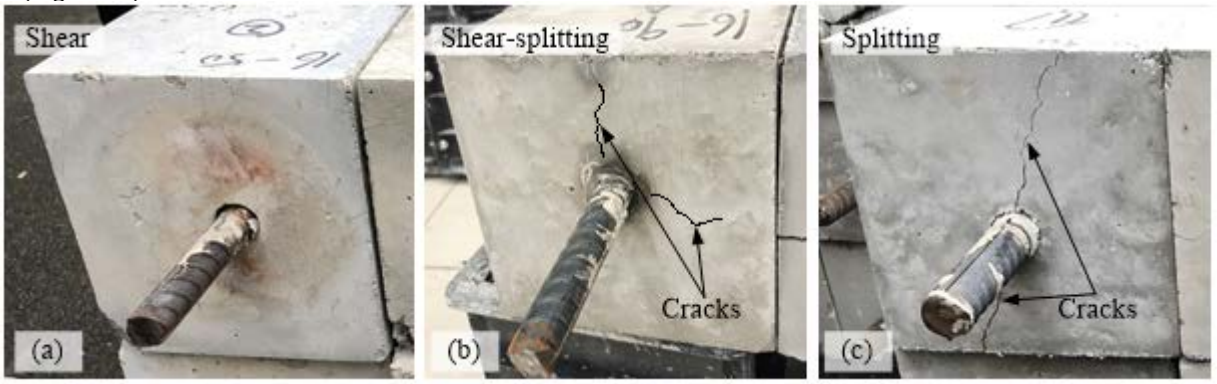

Fig. 8. Failure modes of specimens after pull-out tests (a)Shear (b)Shear-splitting (c)Splitting

The main failure modes of the test specimens were listed in Table 3. In general, at relatively low temperatures, shear failure is dominant, and shear-crack failure is not obvious. With the rise of the heating temperature, the split failure becomes dominant since the tensile strength of PP fiber-reinforced cinder concrete is largely reduced.

Table 3 Summary of failure modes of the tested specimens.

Designation	22℃	200℃	400℃	600℃	800℃
C-16-50	Shear	Shear	Shear	Shear	Shear
C-16-70	Shear	Shear	Shear	Splitting	Shear-splitting
C-16-90	Shear	Shear	Shear-splitting	Splitting	Splitting
C-20-50	Shear-splitting	Shear-splitting	Shear-splitting	Splitting	Splitting
C-20-70	Shear-splitting	Splitting	Shear-splitting	Splitting	Splitting
C-20-90	Splitting	Splitting	Splitting	Splitting	Splitting
C-25-50	Splitting	Shear-splitting	Splitting	Splitting	Splitting
C-25-70	Splitting	Splitting	Splitting	Splitting	Splitting
C-25-90	Splitting	Splitting	Splitting	Splitting	Splitting

4.2 Pull force-slip behaviors

Figure 9 shows the pull force-slip curves of some specimens after different heat treatments. The bond strength of each specimen was subsequently calculated from Eq. (2) by using the tested peak load. The bond strengths of three specimens in each group were averaged (Table 4). Since the curves were basically similar, here we only selected some curves. Each bond-slip curve can be divided into three stages.

(1) Linear elastic stage: At the very beginning of each curve, the PP fiber-reinforced cinder concrete and rebars cooperatively deform, and the pull is enhanced linearly with the slip.

(2) Slight damage stage: As the traction is enhanced, the damage starts to propagate at the interface and inside the PP fiber-reinforced cinder concrete. Thus, the increasing rate of pull force decreases until 0, and reaches the peak on the pull-out curve.

(3) The severe damage stage: As the slip further increases, the pull-out force after maximization gradually declines until becoming 0.

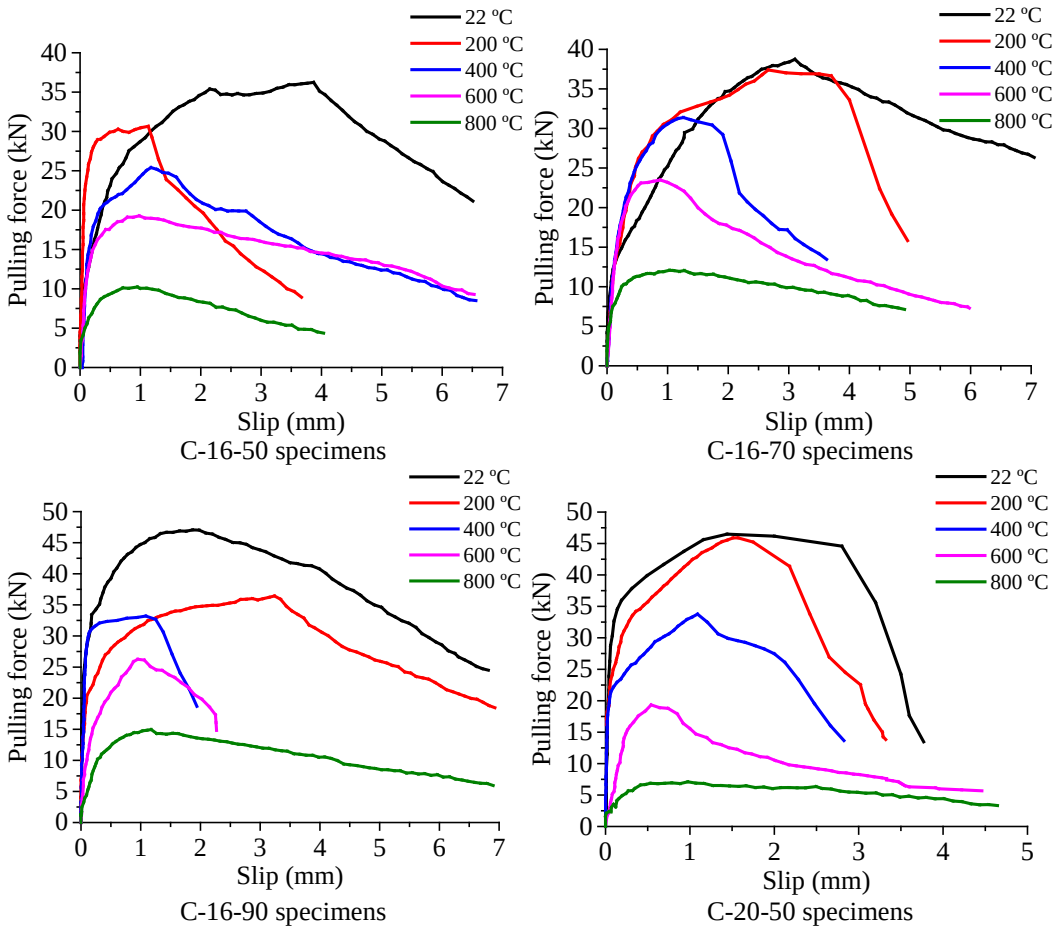

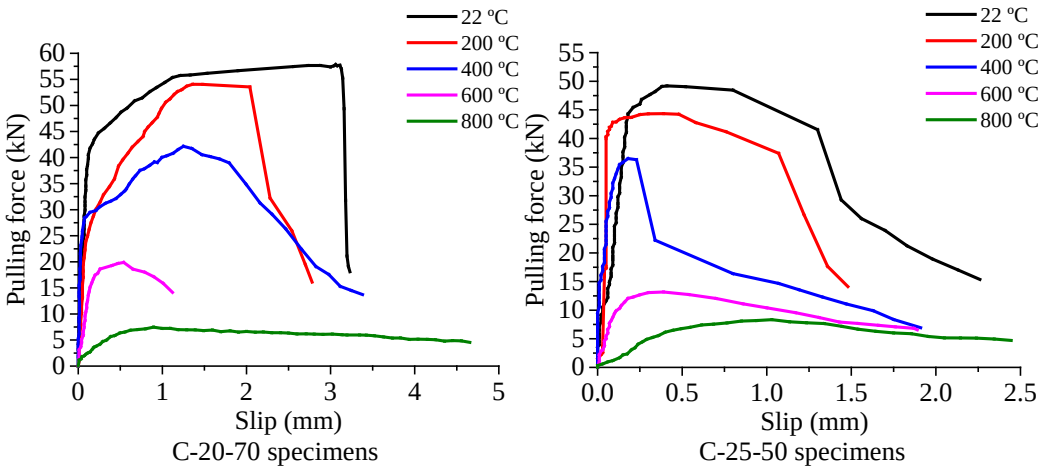

Fig. 9. Pulling force-slip curves of specimens at various temperatures.

As the temperature rises, the internal cement hydrate decomposes and the crack growth due to high-temperature cause the displacement value corresponding to the peak load gradually reduce. However, due to the additional effects of PP fibers melting and decomposing at 200 ℃, the decrease of the displacement value corresponding to the peak load of the specimen is more obvious from 22 ℃ to 200 ℃ (Fig. 9).

The slips of specimens C-16-50, C-16-70 and C-16-90 at peak load ranged from 2.2 to 3.37 mm at 22 ºC, from 1.08 to 1.45 mm at 400 ºC, and from 0.85 to 1.17 mm at 800 ºC.

Table 4 Summary of bond strengths (MPa).

Designation	22℃		200℃		400℃		600℃		800℃	
	Mean	SD	Mean	SD	Mean	SD	Mean	SD	Mean	SD
C-16-50	14.82	0.71	13.07	0.77	10.28	1.29	7.38	1.16	4.12	0.57
C-16-70	11.18	1.03	10.88	1.47	9.65	0.45	6.46	0.59	3.11	1.04
C-16-90	10.45	0.54	8.62	1.52	7.64	1.34	5.41	1.01	2.85	0.39
C-20-50	14.58	0.22	12.99	0.93	10.12	1.53	7.10	1.42	3.16	1.66
C-20-70	10.55	0.89	9.85	1.36	9.14	1.85	5.60	0.57	2.34	1.69
C-20-90	9.07	1.84	8.51	1.28	7.80	1.30	6.09	1.19	2.08	0.70
C-25-50	12.84	0.61	11.05	0.98	9.01	0.62	4.81	1.47	2.49	0.21
C-25-70	10.00	1.29	8.56	1.93	7.52	1.57	4.07	1.40	1.78	0.69
C-25-90	8.09	0.69	7.10	0.43	6.16	1.65	3.56	0.90	1.66	1.13

5. Bond -slip relationship after fire

Based on the pull force-slip curves obtained from the experiments, according to the Eq. (2) and combined with the internal rebar diameter and the bonding length of the specimens, the data of each point in the tensile-displacement curve of 135 specimens were calculated. Further, the bond stress-slip curve of each specimen was obtained. The test data of all the specimens considering different variables at the same test temperature were used to fit the pull force-slip curves. For example, all the tensile and displacement data of C-16-50, C-16-70, C-16-90, C-20-50, C-20-70, C-20-90, C-25-50, C-25-70 and C-25-90 at 22 ºC were further calculated as the correspondence between bond stress and slip strain. Finally, the MATLAB was used for piecewise fitting to obtain the constitutive relationship curves of the bond stress-relative slip of PP fiber-reinforced cinder concrete at various temperatures and the corresponding constitutive Eq. (3)-(17). It can be seen from the figure that as the temperature increases, the bond strength between the rebars and the PP fiber-reinforced cinder concrete was gradually weakened, and the ductility of PP fiber-reinforced cinder concrete was reduced. Due to the factor that majority of PP fibers disappearing when temperature raising, PP fiber-reinforced cinder concrete experiences ductility reduction when temperature increases from 22 ℃ to 200 ℃. When the PP fibers are completely melted and decomposed after 200 ℃, the ductility of the PP fiber-reinforced cinder concrete decreases at a lower rate.

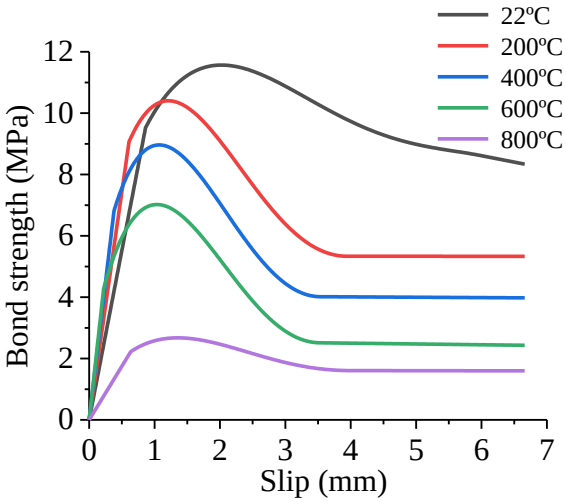

Fig. 10. Bond strength-slip curves at different temperatures.

Based on the test result, the constitutive relationship of bond strength at different temperature were developed:

The constitutive relationship of bond strength at 22ºC

$$\tau = 11.0465s \qquad 0 \le s < 0.86 \qquad (3)$$

$$\tau = -0.0371s^4 + 0.6629s^3 - 4.1551s^2 + 9.9034s + 3.6702 \qquad 0.86 \le s < 6 \qquad (4)$$

$$\tau = -0.4167s \qquad 6 \le s \qquad (5)$$

The constitutive relationship of bond strength at 200ºC

$$\tau = 14.877s \qquad 0 \le s < 0.61 \qquad (6)$$

$$\tau = -0.1219s^4 + 1.7537s^3 - 8.2479s^2 + 13.133s + 3.7416 \qquad 0.61 \le s < 3.95 \qquad (7)$$

$$\tau = -0.001059s \qquad 3.95 \le s \qquad (8)$$

The constitutive relationship of bond strength at 400ºC

$$\tau = 17.9605s \qquad 0 \le s < 0.38 \qquad (9)$$

$$\tau = -0.1611s^4 + 2.1439s^3 - 9.1993s^2 + 13.121s + 3.0406 \qquad 0.38 \le s < 3.54 \qquad (10)$$

$$\tau = -0.0119097s \qquad 3.54 \le s \qquad (11)$$

The constitutive relationship of bond strength at 600ºC

$$\tau = 19.3182s \qquad 0 \le s < 0.22 \qquad (12)$$

$$\tau = -0.1366s^4 + 1.8269s^3 - 7.8188s^2 + 10.928s + 2.2165 \qquad 0.22 \le s < 3.53 \qquad (13)$$

$$\tau = -0.0259188s \qquad 3.53 \le s \qquad (14)$$

The constitutive relationship of bond strength at 800ºC

$$\tau = 3.4961s \qquad 0 \le s < 0.64 \qquad (15)$$

$$\tau = -0.0292s^4 + 0.4281s^3 - 2.0807s^2 + 3.5715s + 0.6883 \qquad 0.64 \le s < 4 \qquad (16)$$

$$\tau = -0.0303688s \qquad 4 \le s \qquad (17)$$

6. Results Discussion

6.1 Effects of heating temperature on bond strength

To simplify the effects of temperature on bond strength, the impacts of other parameters were ignored. During the analysis, the data from experiments with the same thread rebar diameter but different contact lengths were categorised together. Each group was denoted with letters and numbers, and the bond strengths of each group were averaged (Fig. 8). For instance, the bond strengths of C-16-50, C-16-70 and C-16-90 were averaged and clustered as C-16.

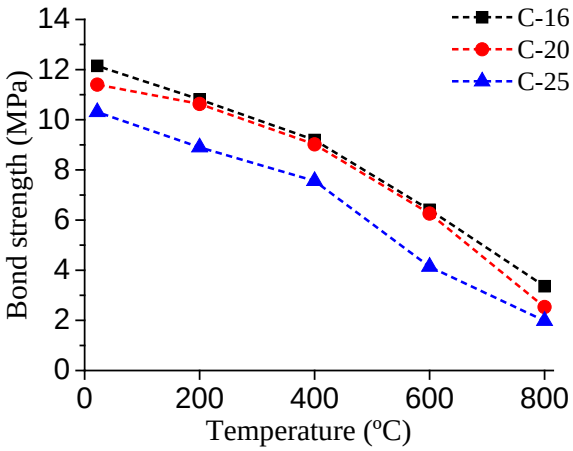

Fig. 11. Effects of heating temperature on bond strength.

With the temperature rising from 22 to 200, 400, 600 and 800 ºC, the bond strengths of C-16 decreased from 12.15 to 10.81, 9.19, 6.41 and 3.36 MPa, respectively, with declining amplitudes of 10.99%, 15.01%, 30.20% and 47.65%, respectively. The bond strengths of C-20 decreased from 11.40 to 10.63, 9.02, 6.26 and 2.53 MPa, respectively, with declining amplitudes of 6.79%, 15.13%, 30.55% and 59.63%, respectively. The bond strengths of C-25 decreased from 10.31 to 8.90, 7.56, 4.14 and 1.98 MPa, respectively, with declining amplitudes of 13.66%, 15.08%, 45.18% and 52.31%, respectively.

The main mechanisms of bond strength reduction are summarized as below:

(1) When the cement hydrates as the interfacial adhesives decompose, the interfacial chemical bond between thread rebars and PP fiber-reinforced cinder concrete is weakened (Arel and Yazici, 2016);

(2) Due to the thermal cracks near the rebar-concrete interface, the chemical bond strength and mechanical interlocking effect will decrease at high temperature (Fu et al. 2004). During the heating and cooling processes, the differences of thermal conductivity, specific heat and thermal expansion coefficient between thread rebars and PP fiber-reinforced cinder concrete would induce thermal stress at the rebar-concrete interface;

(3) The reduction of thermal induction of PP fiber-reinforced cinder concrete's mechanical strength will laterally constrain the rebars (Ma, 2019; Pothisiri, 2012).

(4) The melt-out and decomposition of PP fibers reduce the tensile strength and ductility of PP fiber-reinforced cinder concrete. Thus, when the rebars are pulled during the test, the PP fiber-reinforced cinder concrete substrate is prone to cracking.

6.2 Effects of different variables on bond strength

During the pull-out tests, the effects of different factors on bond strength were studied by changing the rebar diameter and bond length. The average bond strengths of the specimens were weakened with the increase of rebar

diameter and the bond length. Thereby, the percentage of bond strength reduction at different temperatures can be determined. As the rebar diameter increase from 16 to 25 mm, the average bond strength of PP fiber-reinforced cinder concrete at 22, 200, 400, 600 and 800 ºC decreased by 15.47%, 17.86%, 17.95%, 35.35% and 41.33%, respectively. As the bond length prolonging from 50 to 90 mm, the average bond strength at 22, 200, 400, 600 and 800 ºC decreased by 15.12%, 17.66%, 17.72%, 35.38%, and 41.14%, respectively.

7. Conclusions

The strength of this new type of PP fiber-reinforced cinder concrete after fire exposure were tested. The microstructure of PP fiber-reinforced cinder concrete and the PP fibre was inspected using scanning electron microscopy. Pull-out tests were also performed after the fire exposure, the bond stress and slip relation of this type of reinforced concrete undergoing different temperatures were obtained. The effects of temperature, rebar diameter and bond length on the behaviour of this type of structure were analysed.

(1) The bond force between rebars and PP fiber-reinforced cinder concrete was gradually weakened with the temperature rising. With the temperature rising from 22 to 800 ºC, the average bond strength was decreased by 76.79% from 11.29 to 2.62 MPa. This result should be taken into consideration for designing the fire resistance or assessing the post-fire performances of steel reinforced concrete structures.

(2) The bond strength between rebars and PP fiber-reinforced cinder concrete was gradually weakened with the increment of rebar diameter and bond length.

(3) The peak load slip of rebars and PP fiber-reinforced cinder concrete during the pull-out tests decreased with the temperature rising, from 3.4 mm at 22 ºC to 0.85 mm at 800 ºC.

(4) The melt-out and decomposition of PP fibers reduce the tensile strength and ductility of PP fiber-reinforced cinder concrete. Thus, when the rebars are pulled during the test, the PP fiber-reinforced cinder concrete substrate is prone to cracking.

(5) Based on the test results and regression analysis of test data using MATLAB, the bond slip constitutive models of C30 PP fiber-reinforced cinder concrete after exposure to different temperature were first time established, which may contribute to future practical application of PP fiber-reinforced cinder concrete.

Acknowledgments

This research was financially supported by the Foundation of China Scholarship Council（no.201805975002）National Natural Science Foundation of China (no. 51678274), Science and Technological Planning Project of Ministry of Housing and Urban-Rural Development of the People's Republic of China（no.2017-K9-047）.The authors wish to acknowledge the sponsors. However, any opinions, findings, conclusions and recommendations presented in this paper are those of the authors and do not necessarily reflect the views of the sponsors.

References：

Ahmed A E, Al-Shaikh A H and Arafat T I. (1992). Residual compressive and bond strengths of limestone aggregate concrete subjected to elevated temperatures. *Magazine of Concrete Research*, **44(159)**: 117-125.

Alireza Afaghi-Darabi, Gholamreza Abdollahzadeh. (2019). Effect of cooling rate on the post-fire behavior of CFST column. *Computers and Concrete*, **23(4)**: 81-294

Arel H.S., Yazici S., (2014) Effect of different parameters on concrete-bar bond under high temperature, *ACI Mater J*. **111(6)**: 633–639.

Chiang C H, Tsai C L and Kan Y C, (2000). Acoustic inspection of bond strength of steel-reinforced mortar sfter exposure to elevated temperatures, *Ultrasonics*, **38(1-8)**:534-536.

Deng, X.-.F., Liang, S.-.L., Fu, F. and Qian, K. (2020). Effects of High-Strength Concrete on Progressive Collapse Resistance of Reinforced Concrete Frame. Journal of Structural Engineering, 146(6), pp. 4020078–4020078

Diederichs U, Schneider U. (1981). Bond strength at high temperatures. *Magazine of Concrete Research*, **33(115)**: 75-84.

Ding Y., Ning,X. Zhang Pacheco-Torgal Y., F., Aguiar J.B., (2014) Fibres for enhancing of the bond capacity between GFRP rebar and concrete, *Constr Build Mater*. **51**: 303-312.

EI-Hawary M M, Hamoush S A. (1996). Bond shear modulus of reinforced concrete at high temperatures. *Engineering Fracture Mechanics*, **55(6)**: 991-999.

El-Hawary M M, Ragab A M, El-Azim A A, and Elibiari S. (1997). Effect of fire on shear behavior of RC beams. *Computers & Structures*, **65(2)**: 281-287.

Fan X. (2015) Preparation of lightweight aggregate concrete composite insulation of external panel and research of performance. *Dissertation, Jilin Jianzhu University.*

Fu Y F, Wong Y L, Tang, C A, Poon C S. (2004) Thermal induced stress and associated cracking in cement-based composite at elevated temperatures—Part I: Thermal cracking around single inclusion. *Cement and Concrete Composites*, **26(2)**.

Fu, F. (2015). Advanced Modeling Techniques in Structural Design. John Wiley & Sons, Ltd. ISBN 978-1-118-82543-3.

Fu, F. (2016a). 3D finite element analysis of the whole-building behavior of tall building in fire. Advances in Computational Design, 1(4), pp. 329–344.

Fu, F. (2016b). Structural Analysis and Design to Prevent Disproportionate Collapse. CRC Press. ISBN 978-1-4987-8820-5.

Fu, F. (2018). Design and Analysis of Tall and Complex Structures. Elsevier. ISBN 978-0-08-101018-1.

Fu, F., Lam, D. and Ye, J. (2008). Modelling semi-rigid composite joints with precast hollowcore slabs in hogging moment region. Journal of Constructional Steel Research, 64(12), pp. 1408–1419

Fu, F., Lam, D., Ye, J., (2010),Moment resistance and rotation capacity of semi-rigid composite connections with precast hollowcore slabs. Journal of Constructional Steel Research, 66(3), pp. 452-461

Ganesan N., Indira,P.V. Sabeena M.V., (2014) Bond stress slip response of bars embedded in hybrid fibre reinforced high performance concrete, *Constr Build Mater*, **50**: 108–115.

Gao, S., Guo, L., Fu, F., Zhang, S.(2017) Capacity of semi-rigid composite joints in accommodating column loss, Journal of Constructional Steel Research, 139, pp. 288-301

GB(2002) GB/T 50081-2002, Standard for test method of mechanical properties on ordinary concrete. GB, China, Beijing.

GB(2007) GB1499.2-2007, Steel for the Reinforcement of Concrete. Part 2: Hot Rolled Ribbed Bars, GB, China, Beijing.

GB(2010) GB 50010-2010, Code for design of concrete structures. GB, China, Beijing.

Gulsan,M. Eren Khamees N, Abdulhaleem, Ahmet E, et al. (2018) Size effect on strength of Fiber-Reinforced Self-Compacting Concrete (SCC) after exposure to high temperatures, *Computers and Concrete*, **21(6)**: 681-695

Guo, L., Liu, Y., Fu, F. and Huang, H. (2019). Behavior of axially loaded circular stainless steel tube confined concrete stub columns. Thin-Walled Structures, 139, pp. 66–76.

Haddad R H, Al-Saleh R J and Al-Akhras N M. (2008) Effect of elevated temperature on bond between steel reinforcement and fiber reinforced concrete. *Fire Safety Journal*, **43(5)**: 334-343.

Hertz K. (1982). The anchorage capacity of reinforcing bars at normal and high temperatures. *Magazine of Concrete Research*, **34(121)**: 213-220.

Huang,L. Chi,Y. Xu L., Chen P., Zhang A., (2016) Local bond performance of rebar embedded in steel-polypropylene hybrid fiber reinforced concrete under monotonic and cyclic loading, *Constr Build Mater*. **103** 77–92.

Ibrahimbegovic Adnan, Boulkertous Amor, Davenne Luc, et al. (2010). On modeling of fire resistance tests on concrete and reinforced-concrete structures. *Computers and Concrete*, **7(4)**: 285-301.

Kang Hyun, Cheon Na-Rae, et al. (2017). P-M interaction curve for reinforced concrete columns exposed to elevated temperature. *Computers and Concrete*, **19(5)**: 537-544

KODUR V K R, CHENG F P, WANG T C, (2003) Effect of strength and fiber reinforcement on the fire resistance of high strength concrete columns [J]. *Journal of Structural Engineering*, **129(2)**: 1-22.

KODUR V K R, WANGT C, CHENG F P, (2004) Predicting the fire resistance behavior of high strength concrete columns [J]. *Cement Concrete Composite*, **26(2)**: 141-53.

Li Weishi. (2018) Study on the impact of the aggregate system on natural volcanic lightweight aggregate concrete performance, *Building Science*, **34(3)**: 76-81

Lie T T. (1994) Fire resistance of circular steel columns filled with bar-reinforced concrete, *Journal of Structural Engineering*, **120(5)**: 1489-1509.

Liu Dianzhong, Wang Fayu, Fu Feng and Wang,He (2017) Experimental research on the failure mechanism of foam concrete with C-Channel embedment, *Computers and Concrete*, **20(3)**: 263-273.

Lü Junli, Dong Yuli, Yang Zhinian. (2012) Experimental study on the deformation of a two-span steel beam in a structural system subjected to fire, *Engineering Mechanics*, **29(3)**: 110—114. (in Chinese)

Ma Guowei, Huang Yimiao, Aslani Farhad, Kim Timothy, (2019). Tensile and bonding behaviours of hybridized BFRP–steel bars as concrete reinforcement. *Construction and Building Materials*, **201**: 62-70

Moetaz M EI-Hawary, Ahmed M Ragab, Ahmed Abd EI-Azim, et al. (1996) Effect of fire on flexural behaviour of RC beams, *Construction and Building Materials*, **10(2)**: 147—150.

Morley P D, Royles R. (1983) Response of the bond in reinforced concrete to high temperatures, *Magazine of Concrete Research*, **35(123)**: 67-74.

MR Jones, McCarthy A. (2005) Preliminary views on the potential of foamed concrete as a structural material. *Magazine of Concrete Research*, **57(1)**: 21-31.

Pineaud A, Pimienta P, Rémond S and Carré H. (2016). Mechanical properties of high performance self-compacting concretes at room and high temperature. *Construction and Building Materials*, **112**: 747-755.

Pothisiri T., Panedpojaman,P. (2010) Modeling of bonding between steel rebar and concrete at elevated temperatures, *Constr Build Mater*. **27**: 130-140.

Qian K*, Liang S. L., Xiong X. Y., Fu F. and Fang Q (2020) “Quasi-static and dynamic behavior of precast concrete frames with high performance dry connections subjected to loss of a penultimate column scenario”, Engineering Structures, 2020, 205, 110115.

R. Royles, P.D. Morley, (1985) Further response of the bond in reinforced concrete to high temperatures, *Mag Concr Res*, **35(124)**: 157–163.

Rabani M. li Bidgo and Saeidifar.M. (2017) Time-dependent buckling analysis of SiO2 nanoparticles reinforced concrete columns exposed to fire, *Computers and Concrete*, **20(2)**: 119-127

Ramamurthy K, (2009) A classification of studies on properties of foam concrete [J]. *Cement and Concrete Composites*, **31**: 388-396.

Royles R, Morley P D. (1983) Further responses of the bond in reinforced concrete to high temperatures, *Magazine of Concrete Research*, **35(124)**: 157-163.

Sadaghian Hamed and Farzam Masood. (2019). Numerical investigation on punching shear of RC slabs exposed to fire. *Computers and Concrete*, **23(3)**: 217-233

SHEN Rong, FENG Lingyun, RONG Kai. (1991) Evaluation of mechanics performance of steel bars high temperature, *Building Science Research of Sichuan*, **2**: 5.

Tang, Chao-Wei, (2017). Strength degeneracy of LWAC and flexural behavior of LWAC members after fire.

Computers and Concrete, **20(2)**: 177-184

Thomas M D A. (2003) Chloride diffusion in high-performance lightweight aggregate concrete, *Aci Special Publication*.

Vakhshouri Behnam and Nejadi.Shami (2017) Compressive strength and mixture proportions of self-compacting light weight concrete. *Computers and Concrete*, **19(5)**: 555-566

Varona F B, Baeza F J, Bru D, & Ivorra S. (2018) Evolution of the bond strength between reinforcing steel and fibre reinforced concrete after high temperature exposure. *Construction and Building Materials*, **176**: 359-370.

Wang Jun-Yan, Chia Kok-Seng, Liew Jat-Yuen Richard, Zhang Min-Hong. (2013) Flexural performance of fiber-reinforced ultra lightweight cement composites with low fiber content. *Cement and Concrete Composites*, **43**: 39-47.

Wang ZF, (2003) Research on high performance lightweight aggregate concrete (HPLC) and its application, *Wuhan University of Technology*.

Weng Y. H., Qian K.*, Fu F., and Fang Q. “Numerical investigation on load redistribution capacity of flat slab substructures to resist progressive collapse”, Journal of Building Engineering,2020, 29, 101109.

WU Bo, TANG Guihe. (2010) State-of-the-art of fire-resistance study on concrete structures in recent years, *Journal of Building Structures*, **31(6)**: 110-121.

XIAO J Z, FALKNER H. (2006) On residual strength of highperformance concrete with and without polypropylene fibres at elevated temperatures, *Fire Safety Journal*, **41(2)**: 115-121.

Xiao J., Hou Y., Huang Z., (2014) Beam test on bond behavior between high-grade rebar and high-strength concrete after elevated temperatures, *Fire Saf J*. **69** 23–35.

Xiao J., Li Z., Xie Q., Shen L., (2016) Effect of strain rate on compressive behaviour of highstrength concrete after exposure to elevated temperatures, *Fire Saf. J*. **83** 25–37.

YANG Dong-Lin. (2017) Domestic and Overseas Research and Utilization on Lightweight Aggregate Concrete Prepared with Scoria. *The World of Building Materials*, **38(02)**: 26-30

Yang H., Lan W., Qin Y., Wang J., (2016) Evaluation of bond performance between deformed bars and recycled aggregate concrete after high temperatures exposure, *Constr Build Mater*. **112**: 885–891.

YANG Xu, LU Zhoudao, YU Jiangtao, et al. (2014) Simulation of post-fire structural performance of reinforced concrete framesased on the fiber beam mode. *Structural Engineers*, **30(6)**: 33.

Yoo D Y, Kwon K Y, Park J J, & Yoon Y S. (2015). Local bond-slip response of gfrp rebar in ultra-high-performance fiber-reinforced concrete. *Composite Structures*, **120**: 53-64.

ZHENG Wenzhong, YAN Kai, WANG Ying. (2011) Progress in fire resistance of prestressed concrete structures. *Journal of Building Structures*, **32(12)**: 52－61.